

Linking optimization and ecological models in a decision support tool for oyster restoration and management

E. W. NORTH,^{1,6} D. M. KING,² J. XU,³ R. R. HOOD,¹ R. I. E. NEWELL,¹ K. PAYNTER,⁴ M. L. KELLOGG,⁴
M. K. LIDDEL,⁴ AND D. F. BOESCH⁵

¹University of Maryland Center for Environmental Science Horn Point Laboratory, P.O. Box 775, Cambridge, Maryland 21613 USA

²University of Maryland Center for Environmental Science Chesapeake Biological Laboratory, 1 Williams Street, Solomons, Maryland 20688 USA

³Coast Survey Development Laboratory, Office of Coast Survey, National Oceanic and Atmospheric Administration, 1315 East-West Highway, SSMC3, N/CS13, Silver Spring, Maryland 20910 USA

⁴University of Maryland Center for Environmental Science and Department of Biology, College Park, Maryland 20742 USA

⁵University of Maryland Center for Environmental Science, 2020 Horns Point Road, Cambridge, Maryland 21613 USA

Abstract. Restoration of ecologically important marine species and habitats is restricted by funding constraints and hindered by lack of information about trade-offs among restoration goals and the effectiveness of alternative restoration strategies. Because ecosystems provide diverse human and ecological benefits, achieving one restoration benefit may take place at the expense of other benefits. This poses challenges when attempting to allocate limited resources to optimally achieve multiple benefits, and when defining measures of restoration success. We present a restoration decision-support tool that links ecosystem prediction and human use in a flexible “optimization” framework that clarifies important restoration trade-offs, makes location-specific recommendations, predicts benefits, and quantifies the associated costs (in the form of lost opportunities). The tool is illustrated by examining restoration options related to the eastern oyster, *Crassostrea virginica*, which supported an historically important fishery in Chesapeake Bay and provides a range of ecosystem services such as removing seston, enhancing water clarity, and creating benthic habitat. We use an optimization approach to identify the locations where oyster restoration efforts are most likely to maximize one or more benefits such as reduction in seston, increase in light penetration, spawning stock enhancement, and harvest, subject to funding constraints and other limitations. This proof-of-concept Oyster Restoration Optimization model (ORO) incorporates predictions from three-dimensional water quality (nutrients–phytoplankton–zooplankton–detritus [NPZD] with oyster filtration) and larval transport models; calculates size- and salinity-dependent growth, mortality, and fecundity of oysters; and includes economic costs of restoration efforts. Model results indicate that restoration of oysters in different regions of the Chesapeake Bay would maximize different suites of benefits due to interactions between the physical characteristics of a system and nonlinear biological processes. For example, restoration locations that maximize harvest are not the same as those that would maximize spawning stock enhancement. Although preliminary, the ORO model demonstrates that our understanding of circulation patterns, single-species population dynamics and their interactions with the ecosystem can be integrated into one quantitative framework that optimizes spending allocations and provides explicit advice along with testable predictions. The ORO model has strengths and constraints as a tool to support restoration efforts and ecosystem approaches to fisheries management.

Key words: Chesapeake Bay; *Crassostrea virginica*; eastern oyster; ecosystem approach to management; modeling; optimization; restoration.

INTRODUCTION

Restoration of ecologically important marine species and habitats, and implementation of ecosystem approaches to management, present logistical challenges that need quantitative solutions. Restoration is restricted by funding constraints and hindered by lack of

information about trade-offs among restoration goals and about the effectiveness of alternative restoration strategies (Hobbs and Harris 2001, Mann and Powell 2007). Because ecosystems provide diverse human and ecological benefits, achieving one restoration or management objective may take place at the expense of other objectives. This creates difficulties when attempting to allocate limited resources to achieve multiple benefits, when attempting to define and measure restoration success, and when making fisheries management decisions that impact both harvest and ecosystem function.

Manuscript received 15 October 2008; revised 3 June 2009; accepted 9 June 2009. Corresponding Editor: M. J. Vander Zanden.

⁶ E-mail: enorth@hpl.umces.edu

We developed an integrative quantitative tool, the Oyster Restoration Optimization (ORO) model, for the practical implementation of an ecosystem approach to restoration and fisheries management. "An ecosystem approach to management is management that is adaptive, specified geographically, takes into account ecosystem knowledge and uncertainties, considers multiple external influences, and strives to balance diverse social objectives" (National Oceanic and Atmospheric Administration 2005). The ORO model links ecosystem characteristics (hydrodynamics, phytoplankton growth, oyster filtration, oyster population dynamics) with social objectives (improved water quality, harvest, spawning stock sanctuaries, economic considerations) in an optimization framework that provides spatially-explicit information to support restoration and management decisions. The tool is illustrated by examining restoration options related to a single species, the eastern oyster (*Crassostrea virginica*), which supported an historically important fishery in Chesapeake Bay, USA, and provides a range of ecosystem services (National Research Council Committee on Nonnative Oysters in the Chesapeake Bay 2004).

Restoration of eastern oyster populations in Chesapeake Bay is a high priority goal of regional scientific and management communities (Chesapeake 2000 Agreement; information *available online*).⁷ Potential benefits include support of a revived commercial fishery, improved water quality through oyster filtration (Newell et al. 2005), and enhanced fish habitat through reef restoration (Harding and Mann 2001). Efforts to restore *C. virginica* are on-going in Chesapeake Bay. Although Bay-wide oyster populations are not flourishing and disease-related mortality rates are still high (National Research Council Committee on Nonnative Oysters in the Chesapeake Bay 2004), there has been success at some restoration sites (e.g., Brumbaugh et al. 2000, Rodney and Paynter 2006). In addition, numerical model simulations indicate that restoration of oyster populations in tributaries could have a notable impact on water quality in tributaries (Cercio and Noel 2007, Fulford et al. 2007; J. Xu, R. R. Hood, E. W. North, and R. I. E. Newell, *unpublished manuscript*). Yet, the effectiveness of eastern oyster restoration activities in Chesapeake Bay has been questioned due to lack of clarity in objectives and well-defined measures of success (Coen et al. 2007, Mann and Powell 2007). A quantitative approach is needed to support spatially explicit restoration decisions, incorporate costs as well as the ecosystem services provided by oysters, and quantify trade-offs associated with alternative restoration strategies.

The population dynamics of *C. virginica* in Chesapeake Bay are strongly influenced by water circulation patterns and changes in salinity (0 to ~28

psu from the head to the mouth of the estuary). Chesapeake Bay is a large (~300 km long), partially mixed estuary with a persistent halocline and predominantly two-layer circulation patterns (Pritchard 1952, Wang 1979). River inflow influences salinity distributions, which in turn affect the distribution of oysters: adults are generally found in salinities >5 psu throughout the Chesapeake Bay and tributaries (Kennedy 1991). Salinity influences growth (Shumway 1996), disease mortality of adults (Calvo et al. 2001), and larval mortality (Davis and Calabrese 1964). In addition to river flow, the Chesapeake mainstem and tributaries are influenced by tides (0.3–0.9 m tidal amplitude; Schubel and Pritchard 1987, Zhong and Li 2006) and by winds that act both locally and remotely (Boicourt 1992, Li et al. 2005). These circulation patterns alter the flushing time of water in tributaries (Shen and Wang 2007) and the transport and dispersal of oyster larvae (North et al. 2008). Quantifying the spatially complex, and often nonlinear, interactions between physical conditions and oyster populations is essential for guiding and understanding the effectiveness of restoration and management strategies.

Our objective was to create a flexible ecosystem-based decision-making tool to support oyster restoration and management. This paper presents a first "proof of concept" model that links physical, biological, and economic optimization models to provide quantitative information about the ecosystem benefits associated with spatial strategies in oyster restoration. The restoration activities that are the focus of this modeling effort are the placement of hatchery-reared juvenile oysters. We describe here the model formulation and present examples of model predictions to demonstrate the utility of this approach. The new methodology provides a path toward a quantitative structure that, with some improvements, shows promise as a useful tool to support an ecosystem approach to oyster restoration and fishery management.

METHODS

The Oyster Restoration Optimization (ORO) model focuses specifically on predicting how the enhancement of natural oyster populations with hatchery-reared juvenile "seed" oysters influences the ecosystem services provided by oysters in specific regions. The ORO model is a decision support tool that (1) tracks the growth and mortality of hatchery-produced oysters placed at different sites, (2) estimates benefits (e.g., improved water quality, harvest, spawner production), and (3) determines the optimum locations to place oysters that maximize desired benefits given relevant constraints. It incorporates predictions from three-dimensional hydrodynamic, water quality (NPDZ), and larval transport models, calculates size- and salinity-dependent growth, mortality, and fecundity of oysters, and incorporates economic costs of restoration efforts. An optimization approach is used to identify the locations where oyster

⁷ (<http://www.chesapeakebay.net/agreement.htm>)

restoration efforts maximize the weighted sum of potential benefits. The iterative solution technique provided by the RISKOptimizer program (Version 1.0.8; Palisade Corporation, Ithaca, New York, USA), an Excel add-on, allows the incorporation and estimation of uncertainty associated with environmental variability and biological variables. We describe the overall ORO model structure and the optimization solution technique, and illustrate how they can be used to identify trade-offs associated with oyster restoration decisions.

Model structure

Domain.—The ORO model incorporated predictions from sub-models with different space and time scales. Physical conditions (salinity, temperature) and ecosystem services related to oyster filtration and spawning production were projected with hydrodynamic, water quality, and larval transport models that have domains that span the entire Chesapeake Bay (Fig. 1) and had time steps on the order of minutes (<6 min). In specific regions (Fig. 1), the change in abundance and size of seed oysters placed in each region were tracked in annual time increments, from seed oysters (Year 0) to 5-yr-old adults. Fifteen specific regions that span three salinity zones (Fig. 2) were incorporated into this “proof of concept” version of the model for computational efficiency and development purposes. The boundaries of these regions were the same as the boundaries of the hydrodynamic model grid cells.

Control variable.—The ORO model optimizes the number of seed oysters placed in each region. Restoration managers use a constant target placement density (here set to 300 oysters m⁻²) and specify their goals in terms of the area of bottom covered by seed oysters. The ORO model therefore expressed the control variable (the variable to be adjusted and optimized) as the area (*A*) in acres (1 acre = 0.405 hectare) of seed oysters, which was related to number of seed oysters placed (*N*) by

$$N = A \times 4050 \text{ m}^2/\text{acre} \times 300 \text{ oysters/m}^2. \quad (1)$$

It should be noted that, while model calculations were conducted in metric units, all input and output quantities were expressed in units most commonly used in oyster restoration and management efforts within the Chesapeake region (e.g., acres of habitat, bushels of oysters) to facilitate the application of ORO results to these efforts.

Benefits.—Oyster restoration efforts can have the objective of enhancing one or more of the ecosystem benefits that oysters provide. In ORO, the ecosystem benefits of oysters in each region were characterized using measures (e.g., seston reduction, increased sub-surface irradiance, spawning stock production) known to be leading indicators of ecosystem benefits (e.g., water quality, increased production of seagrass, oyster population increase). Harvest was the only model output that was assumed to be a direct benefit measure. All benefit

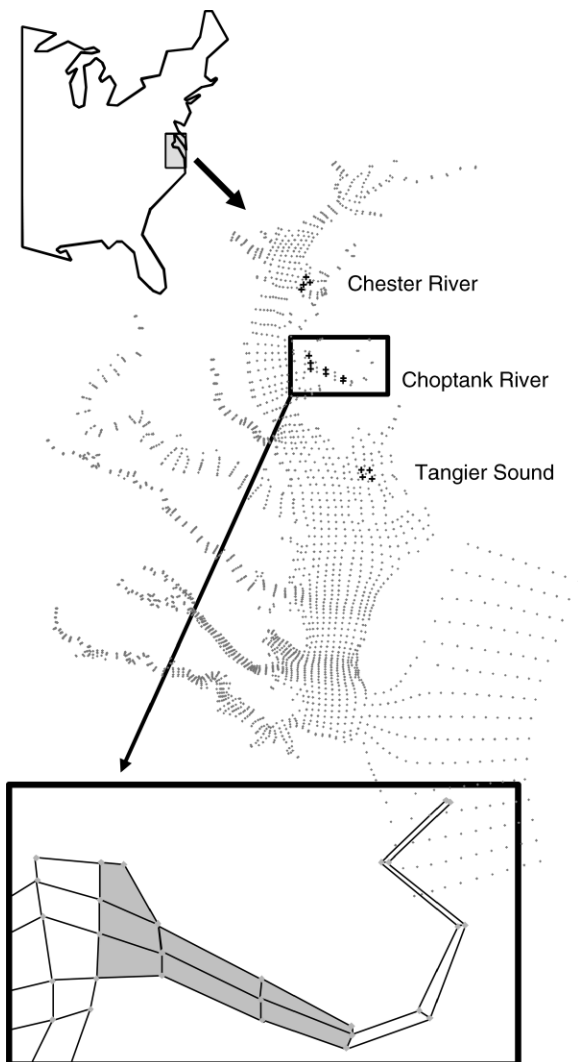


FIG. 1. Location (Chesapeake Bay, USA) and domain of the Oyster Restoration Optimization (ORO) model. Chesapeake Bay hydrodynamic and water quality model grid points are indicated by small gray diamonds. Black crosses in Tangier Sound and the Chester and Choptank Rivers indicate the 15 regions where the ORO model predicts the influence of enhanced oyster abundances. The lower panel shows the shape of the model grid cells in the Choptank River (quadrangles); the gray shading indicates those grid cells in which enhanced oyster abundances and associated benefits were calculated.

measures were based on the number and size of oysters in each region during each year following their placement. These year- and region-specific benefits were summed to determine the total cumulative benefit (*B*):

$$B = \sum_{i=1,15} \sum_{y=1,5} b_{i,y} \quad (2)$$

where *b* = benefit, *i* = region, and *y* = year. The following benefits were calculated in ORO: *R*_{loc}, seston reduction in the local region (mg/L); *R*_{rem}, seston reduction near the (remote) mainstem Chesapeake Bay (mg/L); *L*,

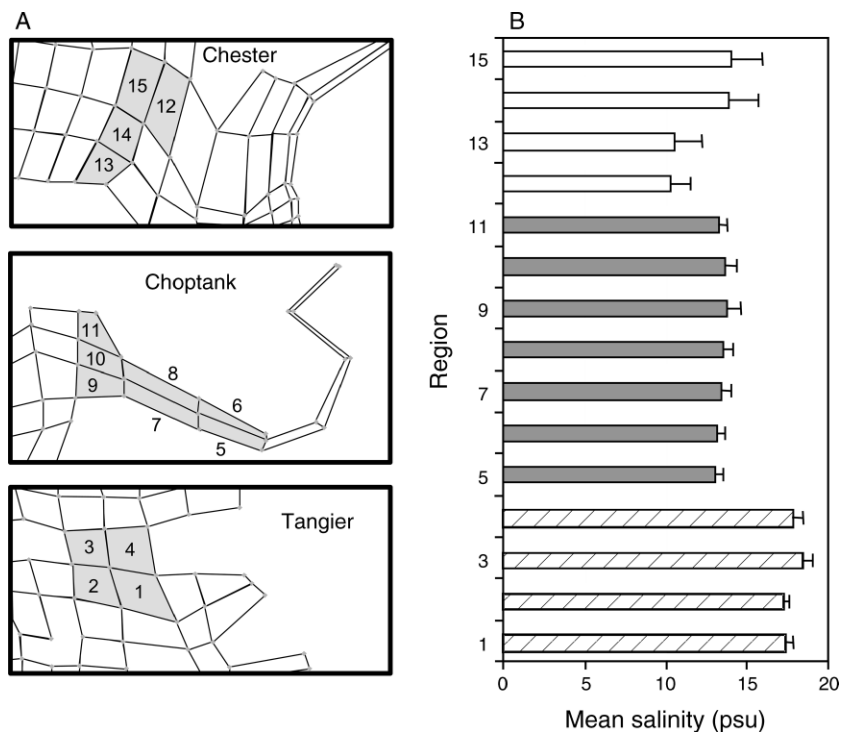


FIG. 2. (A) ORO model regions and (B) salinity (mean and standard error) in each region from May through September 1995. Bars are coded by river system (white, Chester River; gray, Choptank River) or sound (hatched, Tangier Sound). Salinity values were derived from the Curvilinear Hydrodynamics in 3-Dimensions (CH3D) hydrodynamic model at locations indicated by black crosses in Fig. 1. ORO model regions are defined by the hydrodynamic model grid cells.

increased subsurface irradiance in the region at 2 m depth, a critical depth for seagrass growth (watts/m^2); S , spawning stock production index based on larval production and adult survival estimates; and H , harvest (number of bushels, the quantity of trade in the commercial fishery, roughly 0.046 m^3).

The benefits calculated in the ORO model integrated the predictions of a suite of physical and ecological sub-models. Changes in seston concentrations (R_{loc} , R_{rem}) and consequent subsurface irradiance (L) induced by oyster filtration were calculated with a coupled hydrodynamic-water quality model with an oyster filtration and biodeposition sub-model. The benefit of spawning stock production (S) was calculated using information from a demographic model, fecundity estimates, and a larval transport model. The harvest benefit (H) was calculated as a simple proportion of the abundance of oysters once their size was greater than the minimum shell height for legal harvest ($>7.6 \text{ cm}$). Information about specific benefits calculations is described in *Model components and benefits*. Although not included in this version of the ORO model, the benefit of enhanced secondary production related to reef community formation and associated increase in biomass of fish (i.e., recreational fisheries) is under development.

Constraints.—The ORO model predicted the optimum spatial allocation of seed oysters that maximizes a weighted sum of benefits subject to a set of specific

constraints. The major constraints in the model were (1) the maximum number of seed oysters could not exceed hatchery-raised seed oyster production capacities and (2) the costs of restoration (e.g., seed oysters and site preparation costs) could not exceed the funds available. The costs to supply and spread a layer of old oyster shell as site preparation prior to placement of the juvenile oysters were assumed to be US\$10 745 and US\$9 670 per acre for sites <16 acres or >16 acres, respectively, and US\$12 141 per acre for hatchery reared juvenile oysters placed at a density of 1.2 million per acre. In addition, the model solution was constrained by the amount of available oyster habitat in each region. Model solutions that violated these constraints were rejected. The model then searched the range of feasible model solutions for those that maximized the weighted sum of benefits.

Model components and benefits

All benefits calculated in the ORO model relied on predictions from the hydrodynamic model (for salinity and temperature) and the juvenile/adult demographic model (for size and abundance of oysters). These model components are described, as are the methods for calculating the five benefits (R_{loc} , R_{rem} , L , S , and H).

Hydrodynamic model.—We used the coarse resolution CH3D (Curvilinear Hydrodynamics in 3-Dimensions) as the physical sub-model because the model was accessible, already linked to a biogeochemistry model, validat-

ed (Xu and Hood 2006; J. Xu, R. R. Hood, E. W. North, and R. I. E. Newell, *unpublished manuscript*) and computationally efficient. The implementation of CH3D (Xu et al. 2002) had 19 vertical levels to model the circulation and hydrography of Chesapeake Bay (Fig. 1). CH3D is a free surface, three-dimensional, z-coordinate, hydrodynamic model (Sheng 1986) adapted by the U.S. Waterways Experiment Station (WES) for application to Chesapeake Bay (Johnson et al. 1991, Wang and Chapman 1995). Essential hydrodynamic features, such as the two-layered circulation in the main channel and major tributaries, and temperature and salinity structures, can be reproduced by the model (Johnson et al. 1991, Hood et al. 1999, Xu et al. 2002). We used wind, freshwater flow, open ocean tides, and surface heat flux during 1995 to force the hydrodynamic model. Comparison of hydrodynamic model predictions with observations in 1995 indicated that the model was able to simulate spatial and seasonal patterns in hydrography (E. North, J. Xu, R. R. Hood, R. I. E. Newell, D. F. Boesch, M. W. Luckenbach, K. Paynter, *unpublished manuscript*). During this year, annual mean freshwater water inflow to the Chesapeake was below average (1838 m³/s) compared to a 48-yr mean (2195 m³/s with a standard deviation of 548 m³/s; data available online).⁸ The hydrodynamic model made predictions of 3D hydrographic properties (salinity, temperature) and solute transport (suspended sediment, phytoplankton, and so on) for the water quality model. The mean of near-bottom salinity (Fig. 2) and temperature in each grid cell (region) during the oyster growing season (May–September) were calculated for use in the juvenile/adult oyster demographic model, as was the standard deviation of near-bottom salinity in each cell.

Juvenile/adult demographic model.—The change in abundance and shell height of seed oysters placed on bottom in each region were tracked in annual time increments, from seed oysters (Year 0) to 5-yr-old adults using salinity-dependent mortality and growth functions. The change in abundance of oysters from year to year was calculated with size- and salinity-dependent annual mortality rates that were derived from in situ observations of recent “boxes” (shells of recently deceased oysters; Vølstad et al. 2008). Mean and standard deviation of the mortality rates were calculated for two size classes (<5.1 cm and >5.1 cm shell height) and three salinity classes (<11, 11–15, >15). The standard deviation incorporates the variability associated with different disease intensities within each salinity and size class. The change in size of oysters from year to year was calculated with an adaptation of a Von Bertalanffy growth model (Liddel 2008), which includes salinity and temperature as key determinants of the growth constant (*k*) and was derived from in situ observations in Chesapeake Bay. Shell height at Year 0 was set to 25

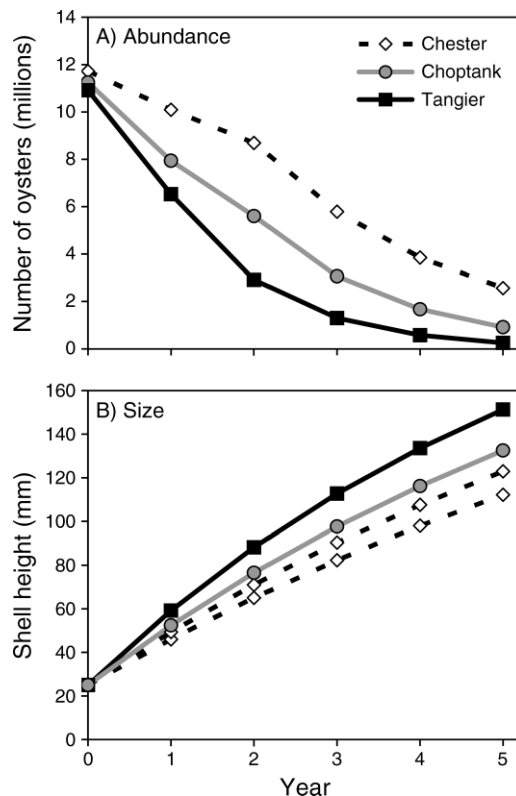


FIG. 3. Example predictions of juvenile and adult mortality and growth in the oyster demographic model. (A) Changes in abundance of seed oysters on a one-acre (0.40 ha) restoration site in the Chester, Choptank, and Tangier systems. (B) Change in size (mean shell height) of seed oysters placed in the three systems. Shell height at Year 0 is for hatchery seed oysters in the fall after having been spawned in the summer. Mean shell height in the Chester River is represented with two lines to show the differences in growth between the high and low salinity regions within the river.

mm, an estimate of the size of hatchery seed oysters in the fall after having been spawned in the summer. An example of the growth and mortality model predictions can be found in Fig. 3.

Environmental variability was incorporated into the growth and mortality functions by creating variation in salinity and in mortality rates. For each iteration of the model, a different salinity and mortality rate was calculated by drawing a random number from a normal distribution with mean and standard deviation of salinity (derived from the 1995 hydrodynamic model predictions) and of mortality rate (derived from Vølstad et al. 2008). The RiskNormal function, provided by the RISKOptimizer software package, was used to generate the random numbers.

Benefits: seston reduction and light penetration.—The benefits of (1) seston reduction in the region where the seed oysters were placed (R_{loc} , mg/L), (2) seston reduction near the mainstem Bay (R_{rem} , mg/L), and (3) increased subsurface irradiance in the region at 2 m depth (L , watts/m²) were calculated with information

⁸ <http://md.water.usgs.gov/publications/ofr-68-Bue10/table9.html>

from the juvenile/adult demographic model linked to a water quality model.

Changes in seston concentrations and consequent subsurface irradiance induced by oyster filtration were calculated with a coupled hydrodynamic-water-quality model with an oyster filtration and biodeposition sub-model. The hydrodynamic model was specified above. The water quality model was adapted for application in Chesapeake Bay (Xu and Hood 2006) from a relatively simple nutrients–phytoplankton–zooplankton–detritus [NPZD]-type model described in Hood et al. (2001). The model tracked two nutrient pools: dissolved inorganic nitrogen and dissolved organic nitrogen. The effect of phosphorus limitation on phytoplankton production was parameterized. The model also contained compartments for phytoplankton, heterotrophs, and detritus. Dissolved oxygen was included to simulate anoxia and hypoxia and served as a natural trigger to slow down the respiratory processes of the heterotrophs under hypoxic and anoxic conditions. The model contained an inorganic suspended solid (ISS) pool that did not participate in the biological cycles but did have a direct effect on light attenuation, which in turn modified phytoplankton growth. An empirical bio-optical model was used to estimate the diffuse attenuation coefficient and light penetration in the water column (Xu et al. 2005). With its simple configuration, the coupled model was capable of reproducing the major features in nutrient concentrations, phytoplankton biomass, oxygen concentration, and underwater light attenuation in a complex biogeochemical system in both dry and wet years. Details on the coupled model system were described in Xu and Hood (2006).

An oyster filtration model was implemented within the hydrodynamic and water quality model to remove seston concentrations from the water column based on the number of oysters in each grid cell. Oyster filtration rates depended on water temperature, salinity, and seston concentrations. Base oyster clearance rates ($\text{m}^3 \cdot \text{kg}^{-1} \cdot \text{s}^{-1}$) of 7.6 cm shell height adult oysters (legal harvest size) were modeled as an exponential function of temperature (Newell and Koch 2004, Cerco and Noel 2005, Fulford et al. 2007) and were modified by salinity and seston concentrations to simulate observed salinity- and seston-dependent reductions in oyster filtration (Newell and Langdon 1996, Shumway 1996). The base clearance rate was zero at salinities < 5 psu and was not suppressed at salinities > 12 psu; between salinities of 12 and 5 psu, the base clearance rate was depressed linearly (Shumway 1996). When seston concentrations dropped below 4 mg/L, the base clearance rate was reduced from 100% to 20%. The base clearance rate was zero at seston concentrations > 25 mg/L (Newell and Langdon 1996).

Simulated oysters removed seston (i.e., phytoplankton, heterotrophs, organic detritus, and ISS) in the bottom layer from the modeled water column at the temperature, salinity, and seston-dependent rate. It was assumed that filtered organic material went into

biodeposits (both feces and pseudofeces), as well as excretion and assimilation. All ISS removed by oysters was assumed to be deposited on the sediment surface as pseudofeces. Two arrays of biodeposits, organic and inorganic, were carried for each bottom grid in the model. Organic and inorganic biodeposits were tracked separately so that they could be resuspended either to the organic detritus pool or the ISS pool in the model. The arrays were created to track the age of the biodeposits. For the resuspension processes, biodeposits were divided into three age pools: fresh (0–2 days), medium (2–4 days), and old (> 4 days). A critical shear stress and resuspension rate were applied to each pool. Denitrification occurred in the medium aged pool of biodeposits if the bottom grid was below the euphotic zone, and the total N loss due to denitrification for this pool was set to 20% (Newell et al. 2002).

The spatial distribution of present-day oysters within the model was based on the location and area of public (i.e., natural) oyster bars in Virginia waters and the “cultch” (i.e., oyster shell) GIS layer from the Maryland Bay Bottom Survey (MBBS) reduced by 87.5% to reflect siltation and burial of oyster shell in Maryland waters since the MBBS was conducted (Smith et al. 2001, 2005). The center locations of oyster bar polygons were mapped to the CH3D grid and the area of cultch within each grid cell was summed. Present-day abundances of oysters were based on Chesapeake Bay Oyster Population Estimation (CBOPE) fisheries-independent measurements of oyster biomass from basins in Maryland (2000–2002) and Virginia (2000–2003; data available online).⁹ Biomass estimates (g dry mass of oysters/ m^2) were averaged for each basin, then converted to number of 7.6-cm oysters/ m^2 using the conversion of 1.3 g dry tissue mass per 7.6-cm oyster (Jordan et al. 2002). This procedure converted the biomass of oysters of all sizes to the abundance of 7.6-cm oysters for compatibility with temperature-dependent clearance rate calculations. Although this conversion assumed a linear size vs. filtration rate relationship (which can be nonlinear; Newell and Langdon 1996), it was implemented in order to directly connect the complex NPZD model with other ORO sub-model components. The basin-specific estimate for present-day oyster abundance was assigned to each CH3D grid cell within the appropriate basin.

Repeated runs of the water quality model were used to develop relationships between the number of oysters placed in each region and the change in seston and irradiance levels (Fig. 4). The model was run with present-day abundances of oysters for a baseline. Then, the model runs were repeated with 10 times, 20 times, 50 times, 100 times, and 300 times present-day abundances in each region (15 regions \times 5 runs for each region = 75 model runs). For each run, the depth-averaged seston

⁹ (<http://www.vims.edu/mollusc/cbope/overview.htm>)

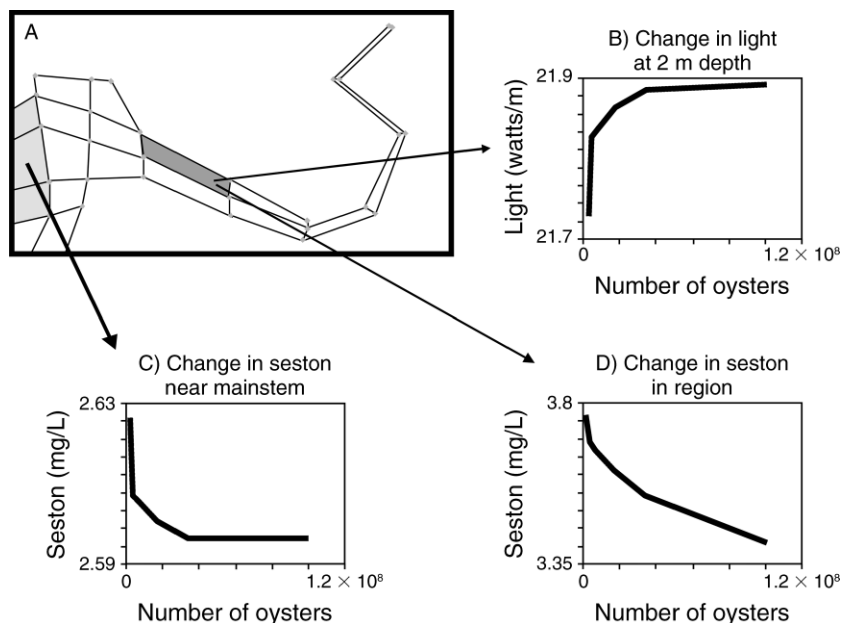


FIG. 4. (A) Modeled regions of the Choptank River and examples of piecewise functions (B–D) used to summarize 3-D ecosystem model predictions for each region. The piecewise functions show the predicted relationship between the number of oysters in a region (dark gray area within Choptank River) and the resulting change in (B) subsurface irradiance, (C) depth-averaged seston concentrations at the mouth of the Choptank River near the mainstem Bay, and (D) depth-averaged seston concentrations within the region. Note the differences in scale. Changes in seston concentrations near the mainstem Bay were calculated using predictions from the 3-D model cells near the river mouth (light gray leftmost cells in panel A).

concentration and subsurface irradiance at 2 m were recorded in hourly intervals and then averaged for the period May to September. This information and piecewise linear regressions were used to develop relationships between 7.6-cm oysters abundance and changes in seston and irradiance in each region for use in the ORO model (Fig. 4). To calculate the benefits within each ORO region, the predictions of the shell height and abundance of oysters placed within each region from the demographic model were converted to the number of standard shell height 7.6-cm oysters. The piecewise linear regressions were then used to calculate the reduction in seston, or increase in irradiance, in each region for each year and summed to derive the total benefit (e.g., Eq. 2).

Benefit: spawning stock production.—The benefit of spawning stock production (S , an index of the relative number of offspring that could survive to age 5) was calculated using information from the demographic model, fecundity estimates, and a larval transport model. The proportion of oysters, which are a sequential hermaphroditic species, that were female in each region and year was calculated with oyster shell height and a linear regression relationship developed from in situ observations in Chesapeake Bay (Fig. 5; L. Kellogg, unpublished data). This proportion was multiplied by the number of oysters in each region and year to determine the number of female oysters. Egg production by these females was calculated using the relationship given by Choi et al. (1993) (Fig. 5) and then multiplied by larval

salinity-dependent mortality (Fig. 6) (Lough 1975) and larval transport success to estimate the number of offspring that survive to find suitable habitat on which to settle. The mortality rates from Year 0 to Year 5 calculated in the demographic model were then applied to the number of surviving offspring to produce an estimate of the number of offspring that could survive to age 5. This index does not incorporate many aspects of larval and early post-settlement mortality (e.g., predation) for which spatially explicit (or salinity-dependent) information was not available. As such, it is not an absolute predictor of the abundance of offspring (i.e., it does not predict recruitment); rather, it provides a quantitative index that allows comparison of potential spawning production between regions.

Larval transport success was calculated with stored output from a Bay-wide oyster larvae transport model (North et al. 2008) which coupled a high-resolution regional ocean model system (ROMS) hydrodynamic model (Li et al. 2005) and a particle tracking model. It predicted the transport of particles from their release to settlement or terminal location, and included the best present-day estimate of oyster habitat and algorithms that gave particles vertical swimming behaviors similar to oyster larvae. Larval transport model simulations were conducted in years with different physical conditions (1995–1999). Transport success, the proportion of particles released from a bar that encountered settlement habitat, was calculated for individual oyster bars (Fig. 7). The transport success scores of individual

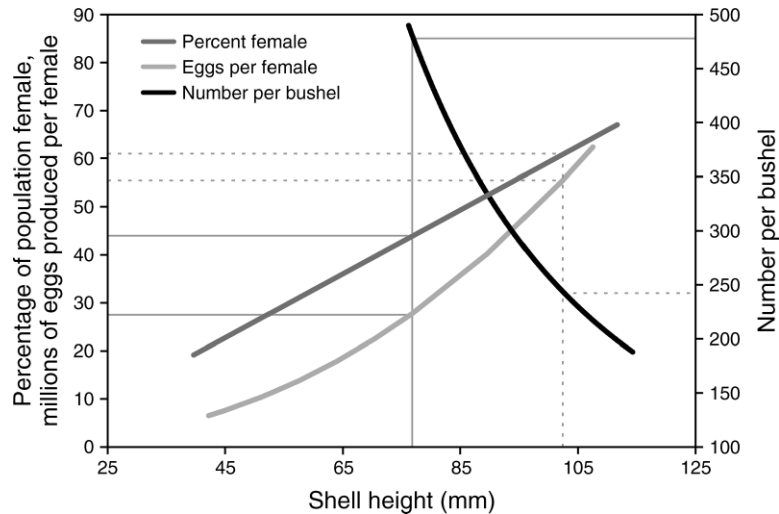


FIG. 5. Size-based relationships that are part of the calculations of spawning production and harvest benefits in the ORO model. The percentage of a population that are females (dark gray line; L. Kellogg, unpublished data) and eggs produced per female oyster (light gray line; Choi 1993) are used in the calculation of offspring produced in each region. The harvest benefit is calculated with the number of oysters in a bushel (1 bushel = 0.046 m³), the unit of commerce (black line; MdDNR Shellfish Division, unpublished data). Solid gray lines indicate predicted values for legal-size oysters (7.6 cm). Dashed gray lines indicated predicted values for oysters that are 10.2 cm in shell height.

bars were averaged within each ORO region to produce an estimate of transport success for use in the ORO model.

Benefit: harvest.—The harvest benefit (*H*, number of bushels) was calculated as a simple proportion of the abundance of oysters once their size was greater than the legal minimum shell height. For the model runs presented here, the proportion harvested was set to 0.2 and the legal minimum shell height was 7.6 cm (the current legal minimum in Chesapeake Bay). The number of harvested oysters in each year was converted into number of bushels using an exponential relationship ($n = 1.37 \times 10^7 sh^{-2.36}$) that converted shell height of oysters (*sh*) to number of oysters per bushel (*n*) (Fig. 5), which was derived from data provided by Maryland Department of Natural Resources Shellfish Division (Chris Judy, personal communication).

Optimization solution technique

The ORO model was used to maximize a single benefit and to maximize a group of benefits. The solution technique involved maximizing the mean of the predicted total benefits (TB), where

$$\begin{aligned}
 TB = & w_1 \sum_{i=1,15} \sum_{y=1,5} R_{loc\ i,y} + w_2 \sum_{i=1,15} \sum_{y=1,5} R_{rem\ i,y} \\
 & + w_3 \sum_{i=1,15} \sum_{y=1,5} L_{i,y} + w_4 \sum_{i=1,15} \sum_{y=1,5} S_{i,y} \\
 & + w_5 \sum_{i=1,15} \sum_{y=1,5} H_{i,y} \tag{3}
 \end{aligned}$$

and *w* = weighting factors (subscripts are defined as in Eq. 2). In the case of maximizing a single benefit, *w* = *a*/*M* where *a* was a user-defined selectivity parameter (*a*

= 1 for the benefit of choice and *a* = 0 for the remaining benefits), and *M* was an estimate of the maximum possible benefit that could result if all available habitat was covered with seed oysters. *M* converted the benefit to a unitless quantity and allowed comparison of benefits by eliminating the orders-of-magnitude differences between individual benefits (e.g., 0.96 mg/L seston reduction vs. 3×10^7 offspring produced). When maximizing a combination of benefits, then $w = ac/M$. In this case, *a* was set to the appropriate proportion (e.g., for equal weighting *a* = 0.2 for all benefits) and a scaling factor (*c*) was used to ensure that benefit values had

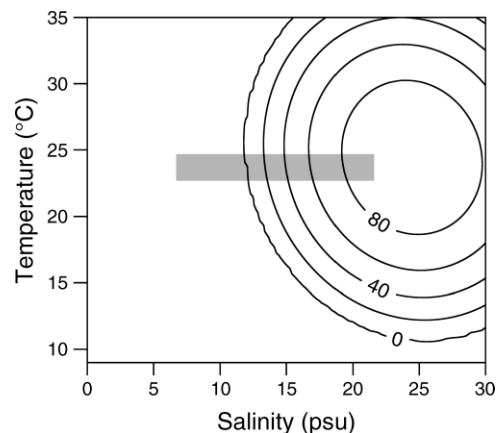


FIG. 6. Survival (%) of *Crassostrea virginica* larvae at different salinity and temperature combinations. This response-surface relationship was redrawn from Lough (1975) and was based on laboratory experiments of Davis and Calabrese (1964). The shaded region represents the range of salinity and temperature values in the ORO model.

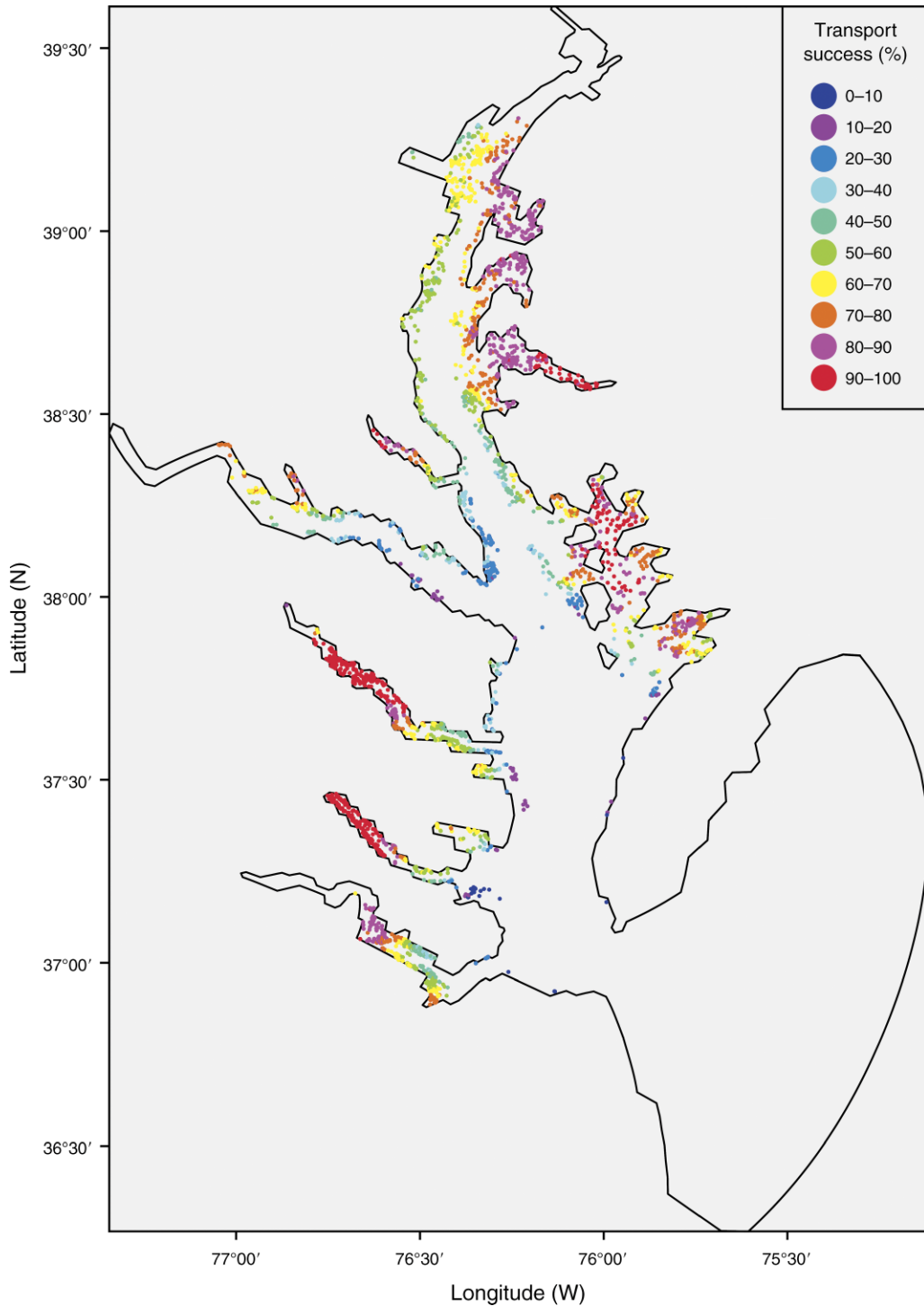


FIG. 7. Transport success scores for individual oyster bars based on larval transport model simulations (1995–1999). Individual oyster bars are color-coded according to the percentage of particles released from the bars that encountered settlement habitat. The transport success scores of individual bars were averaged within each ORO region for use in the ORO model. The outline indicates the boundary of the larval transport model. The figure is reproduced from North et al. (2008).

equal weight when added together. The scaling factors were derived with model runs that maximized each individual benefit separately and were calculated as $c_k = TB_{\max}/TB_k$ where TB_{\max} was the highest TB from all

runs, and TB_k was the highest TB from each individual run that maximized benefit k .

An optimization approach was used to identify the most suitable locations for seed oyster placement that

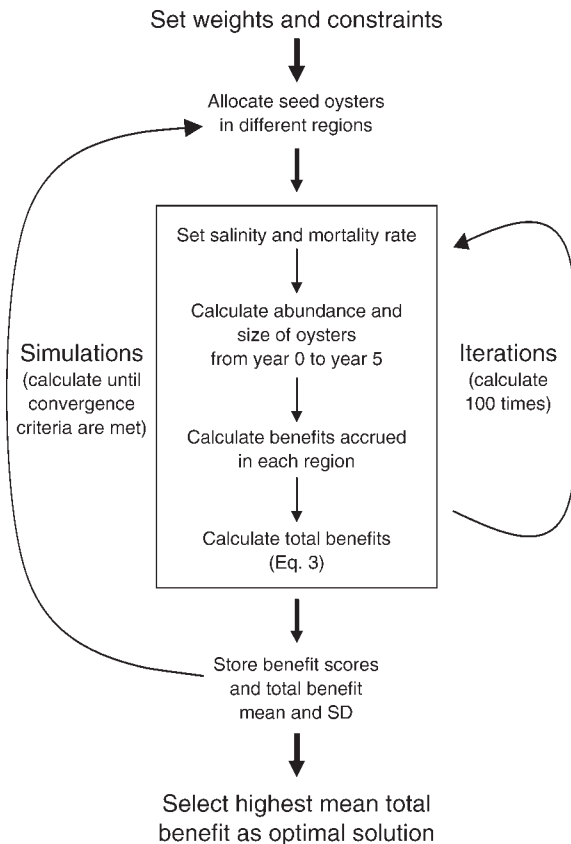


FIG. 8. Flow diagram of model processes. For each model run, constraints and benefit weight values are set. Within each run, simulations with different spatial allocations of oysters were repeated until convergence criteria were met. Within each simulation, 100 iterations were conducted with different values of salinity and adult/juvenile oyster mortality rates to incorporate environmental and biological variability in the model solution.

maximized one or more benefits. The iterative solution technique was provided by Palisade's RISKOptimizer program using the "budget" solving method. For each ORO model run (Fig. 8), simulations were conducted until convergence criteria were met (solution changes less than 0.01% in last 100 simulations). For each simulation, the benefits related to one spatial allocation of seed oysters were calculated (e.g., 5 acres in region 3, 7 acres in region 10, and 14 in region 12, etc.). Within each simulation, 100 iterations were conducted, each with a different salinity and mortality rate. The value of salinity and mortality was assigned by drawing a random number from a normal distribution with mean and standard deviation that was set with model predictions (salinities from the CH3D model) or observations (mortality rates from Vølstad et al. 2008). This iterative solution technique incorporated and estimated uncertainty caused by environmental variability and mortality rates. For each simulation, all iterations that did not meet constraints were excluded and the mean total benefit (TB) score and standard deviation of

acceptable iterations were calculated. Multiple simulations were conducted with an optimization algorithm (a genetic algorithm with mutation rate = 0.7 and crossover rate = 0.2) to restrict the parameter space that was searched (i.e., a limited combination of acres was tested by the model). Hundreds of simulations were conducted, each with a different spatial allocation of seed oysters, until the convergence criteria were met. The solution with the highest mean Total Benefit contained the optimum spatial allocation of seed oysters and an estimate of the associated benefits that could accrue. When the model was run with different weights assigned to various benefit measures, the solutions could differ markedly, especially when the models were optimized for only one benefit measure. These differences provided a quantitative basis for assessing trade-offs related to restoration goals and the strategies needed to achieve them.

To explore the behavior and capabilities of the ORO model, model runs were conducted with each of the five benefits optimized individually ($a = 1$ for the benefit of choice and $a = 0$ for all other benefits) and with all benefits weighted equally ($a = 0.2$ for all benefits). All runs were initialized with the constraints of 50 000 000 seed oysters and US\$1 000 000 budget limit. This translated into 41.2 acres of seed oysters which were initially placed in one region (region 6) to meet a requirement of RiskOptimizer's budget solving method and to ensure adequate parameter search space for the optimization routine. The six model runs conducted represent different restoration strategies, each with a different objective for oyster restoration (e.g., restore water quality in the region, restore water quality in the mainstem Bay, enhance seagrass growth, promote population replenishment, or enhance harvest). Model predictions were examined to determine if the optimal spatial arrangement of seed oysters varied when different benefits were maximized. In addition, all benefits associated with each optimization model run were compared to gain a quantitative understanding of the trade-offs (i.e., hidden costs and unintended benefits) associated with each potential restoration strategy.

RESULTS

The ORO model predicted that the optimum spatial allocation of seed oysters differs depending upon which benefit (or benefits) was maximized (Fig. 9). One region within the Choptank River (region 7) was predicted to be the optimum location to place oysters to (1) maximize seston reduction in the region and near the mainstem Bay (Fig. 9B, D), and (2) maximize all benefits weighted equally (Fig. 9G). The water residence time and oyster filtration capacity in the Choptank River are high (E. North, J. Xu, R. R. Hood, R. I. E. Newell, D. F. Boesch, M. W. Luckenbach, and K. Paynter, *unpublished manuscript*) and likely contribute to the ability of oysters to reduce seston concentrations compared to the other tributary sub-estuaries. When the locations of seed

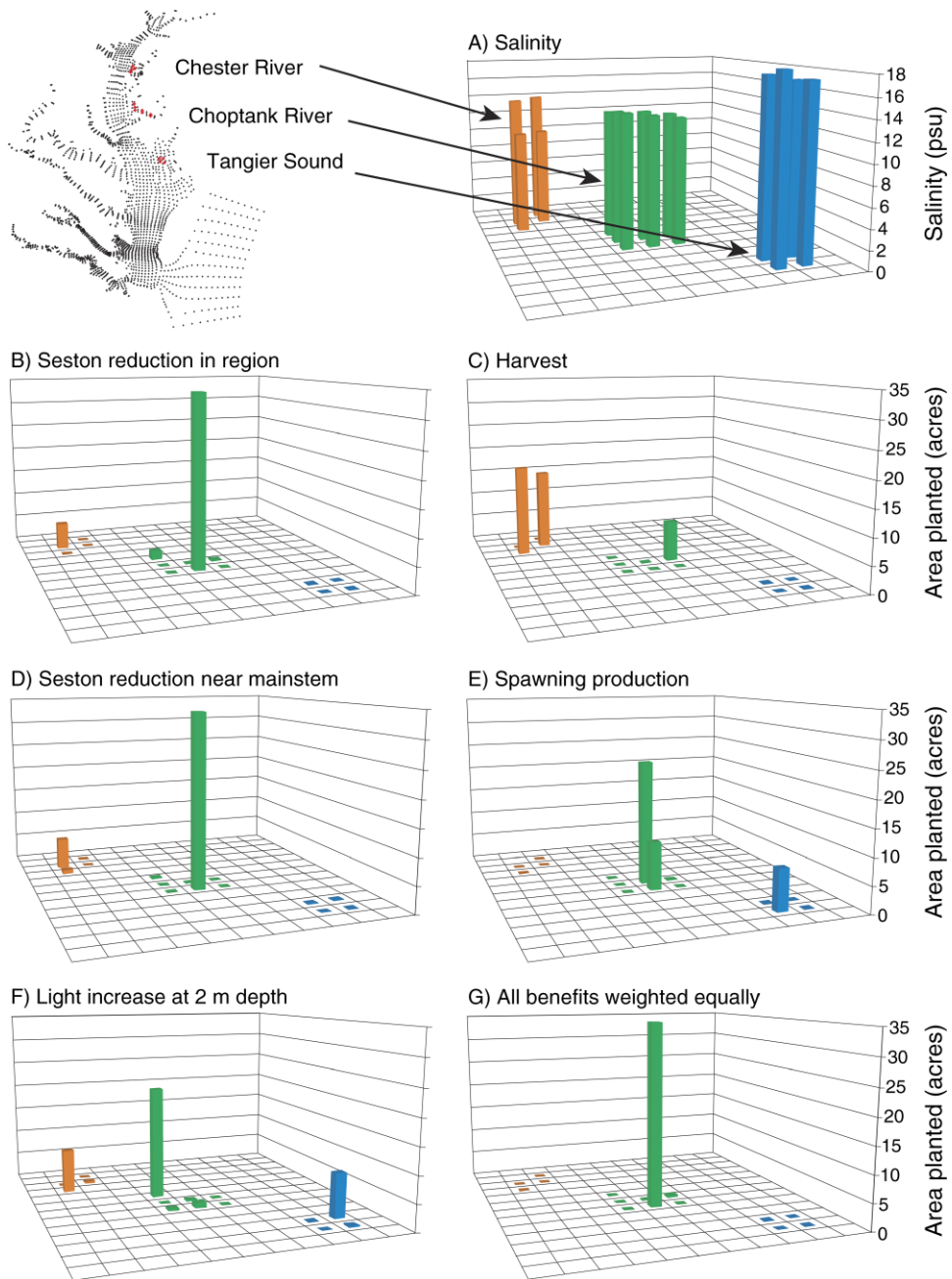


FIG. 9. ORO model predictions of the optimum regions to place seed oysters in order to maximize single or multiple benefits. Each vertical bar represents results for each region, and bars are color coded according to basin (orange, Chester River; green, Choptank River; blue, Tangier Sound). The upper panels show the model domain (upper left panel) and the salinity (panel A) in each of the 15 regions of the ORO model. The remaining panels indicate the optimum spatial allocation of acres of seed oysters when a single benefit is maximized (panels B–F) or all benefits are maximized equally (panel G). Note: 1 acre = 0.40 ha.

oyster placement were optimized to increase subsurface irradiance at 2 m depth, the model recommended placement in three main regions, one in the Choptank River region (region 11), one in the Chester River and one in the Tangier Sound (Fig. 9F). The ORO model predicted that spawning stock production would be maximized if most seed oysters were placed in the middle

reaches of the Choptank River (Fig. 9E), likely because larval transport success scores were high (91–92%) in these regions (regions 7 and 8) and salinities provide a balance between adult disease-related mortality (highest in salinities > 15; Fig. 3) and larval salinity-dependent mortality (which was 100% at salinities < 12 based on Lough [1975]; Fig. 6). In contrast with the other

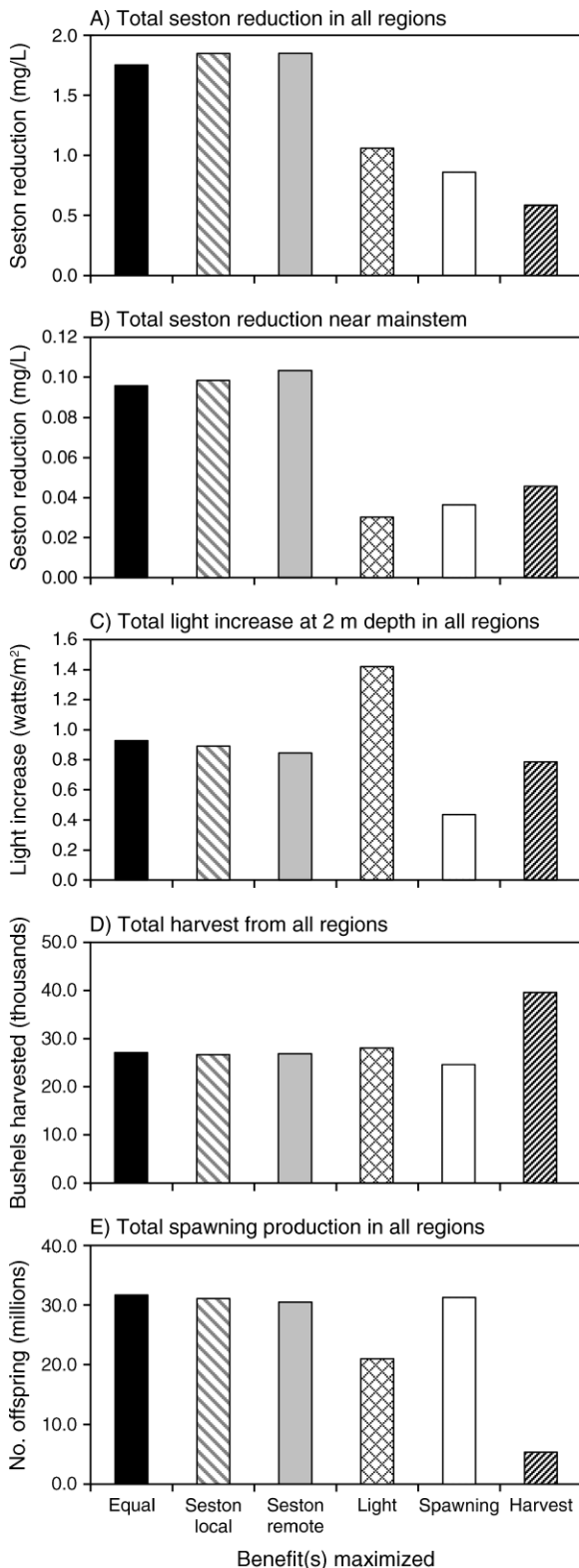


FIG. 10. Cumulative benefits (y -axes) for each spatial allocation of seed oysters that maximizes single or multiple benefit(s) (x -axis categories). The ORO model quantifies benefits in each region and sums them over all regions to compute the total benefits that are associated with the spatial

benefits, the Chester River was the optimum place for maximizing harvest (Fig. 9C), most likely due to low salinities in this region that resulted in low mortality of adults due to diseases. Although growth was slower in these low salinity waters, the low disease mortality in low salinities allowed more oysters to grow to a larger size (Fig. 3). This, combined with the fact that fewer large oysters were needed to fill a bushel (Fig. 5), resulted in enhanced harvest.

The ORO model provides quantitative information about all benefits when an individual benefit or multiple equally weighted benefits were maximized (Fig. 10). For example, all optimization runs result in harvest of $>20,000$ bushels, but optimizing for harvest was predicted to result in harvest of $\sim 10,000$ more bushels than the other runs (Fig. 10D). In addition, ORO model predictions allowed assessment of the trade-offs between restoration strategies. For example, some optimization runs did not result in benefits that were substantially different from other runs. When local reduction in seston was optimized, the number of offspring produced was only slightly lower than the run that maximized spawning stock production (Fig. 10E). Hence, offspring production was an unintended benefit of the restoration strategy to reduce seston. In contrast, some optimization model runs resulted in notably lower benefits than the run designed to optimize a particular benefit. For example, less reduction in seston was apparent when spawning success or harvest was maximized (compare "Spawning" and "Harvest" bars with the "Seston" bars in Fig. 10A, B). The difference between optimizing for harvest and for spawning stock production benefits was notable: optimizing for harvest resulted in a large reduction in the number of offspring produced compared to other optimization configurations (Fig. 10E).

Additional model runs (not presented here) with different starting spatial arrangements of seed oysters indicated that model results were somewhat sensitive to initial conditions. We found that the budget solving method required that all 41.2 acres of seed oysters initially be placed in one region. If the initial acreage of seed oysters was divided among multiple regions, the parameter-space search of the optimization routine was restricted. When model runs were conducted with all 41.2 acres of seed oysters initially in different regions, the results were similar to those presented here in terms of the spatial allocations of seed oysters among systems

← arrangements of seed oysters that would maximize all benefits equally (Equal) or maximize individual benefits: Seston local, seston reduction in the region; Seston remote, seston reduction near the mainstem Bay; Light, increase in subsurface irradiance at 2 m depth; Spawning, spawning stock production (number of offspring produced); and Harvest, number of bushels harvested. This information provides a quantitative assessment of the trade-offs (i.e., hidden costs and unintended benefits) associated with restoration strategies that seek to optimize one or more benefits of the ecosystem services of oysters.

(Chester, Choptank, Tangier), but there were differences in the spatial allocation of seed oysters within each system.

DISCUSSION

The Oyster Restoration Optimization model demonstrates that ecosystem characteristics (hydrodynamics, phytoplankton growth, oyster filtration, oyster population dynamics) and social objectives (water quality, harvest, spawning stock sanctuaries, economic considerations) can be linked in an optimization framework that employs measures of costs and several categories of benefits, and provides spatially explicit information to support oyster restoration and management decisions in Chesapeake Bay. The model incorporates environmental variability and provides information about where to place seed oysters in order to maximize a given benefit or group of benefits. As such, the model does not specify quantitative endpoints/goals, but rather allows the user to weight each benefit to reflect the objectives of a particular project and then calculate the benefits that could be expected to accrue. In addition, it provides a quantitative estimate of the consequences of restoration decisions by calculating the hidden costs and unintended benefits associated with different spatial arrangements of seed oysters. Importantly, it provides quantitative predictions that could be validated with field observations such as size-specific abundance of oysters and seston reduction due to oyster filtration (Grizzle et al. 2008). Once validated, model predictions could be used to help define quantitative success criteria for oyster restoration projects or assess whether or not previously defined restoration targets could be met.

Although numerical modeling is not a new approach in oyster management and restoration, the ORO model combines several classes of models to form a new decision support tool. One-dimensional models have long been used to gain insight on major factors that influence oysters (e.g., Powell et al. 1995, Hofmann et al. 2001); population models have been linked with three-dimensional hydrodynamic models to provide management advice (e.g., Klinck et al. 2002, Cerco and Noel 2007); demographic and habitat suitability models have been used to inform restoration of shellfish in specific locations (McCay et al. 2003, Barnes et al. 2007); a Stoplight Report Card model has been designed to assess the impacts of restoration activities on oyster populations and ecosystems (Volety et al. 2009). The novel contribution of this modeling effort is the integration of demographic, 3-D circulation-ecosystem, and larval transport models within an optimization framework that allows prediction of multiple benefits and the trade-offs between them. The iterative solution technique incorporates uncertainty such as that caused by environmental variability. The model links important nonlinear, and often-competing, biological processes (i.e., Figs. 3, 5, and 6) with their effects on both ecological benefits (water quality, spawning stock

production) and on human use benefits (harvest). This is exemplified in Fig. 5 (gray and dashed lines) which shows the change in sex ratio, egg production, and number of oysters in a bushel when minimum harvest shell height is increased from 7.6 to 10.2 cm, a difference which nearly doubles both the number of eggs produced and nearly halves the number of oysters needed to fill a bushel.

In addition to integrating ecological and human use factors, the ORO model quantifies trade-offs among multiple benefits, and demonstrates that restoring one benefit does not necessarily result in optimum restoration of all benefits (Fig. 10). This information can be used to inform restoration decisions and better define the success of restoration programs. For example, model results indicate that restoration with the objective of maximizing spawning stock production would not be most effective in low salinity waters of Chesapeake Bay, and the number of bushels harvested would not be a good measure of success because high harvest is not associated with optimal spawning production (Fig. 10D, E).

Despite the fact that the ORO model has promise to be a useful tool to support oyster restoration efforts in Chesapeake Bay, its current implementation has some limitations. The resolution of the hydrodynamic and water quality models likely are too low to capture important hydrodynamic features in the Chesapeake that could have a strong influence on water residence time and, subsequently, oyster filtration capacity, such as sub-tributaries with high residence times and bathymetric features that create residual eddies. In addition, the modeled larval salinity-dependent mortality rate (Lough 1975) was based on mortality experiments with Long Island Sound oysters acclimated to higher salinities than those found in the regions of this model (Davis and Calabrese 1964). Because it is likely that larvae produced by oysters in lower salinity waters in Chesapeake Bay are more tolerant of lower salinities (Davis 1958; D. Merritt, *personal communication*), the apparent conflict between optimizing spawning stock and harvest benefits could be exaggerated in the current ORO model predictions. Finally, there are many other aspects that could be incorporated into the modeling framework, including (1) adding the benefit of habitat refuge and trophic transfer to fish (Rodney and Paynter 2006), (2) running the ecosystem/oyster filtration model for additional years with different environmental forcing (e.g., with high and low freshwater flow) to better capture environmental variability, (3) accounting for quantity of surficial shell substrate created or lost (Powell et al. 2006), (4) refining larval and early post-settlement mortality estimates, (5) predicting multiple generations of offspring production, (6) adding size-specific oyster populations and filtration rates to the NPZD model (Newell and Langdon 1996), and (7) incorporating recent experimental work on resuspension

of oyster biodeposits to NPZD model parameterizations (Holyoke 2006).

Although there are many options for improving this decision support tool, we think that the next steps for ORO model enhancement include (1) implementing it with higher resolution hydrodynamic and water quality models, (2) adding salinity-dependent larval mortality rates for Chesapeake oysters discerned from laboratory experiments, (3) conducting model-data validation studies of the juvenile/adult demographic model, and (4) transferring the model into a compiled computer language for greater computational efficiency. The preset algorithms, spreadsheet format, and embedded graphics makes Palisade Corporation's RISKOptimizer an excellent software package for the initial development of this complex and integrated model. However, because the integrated biophysical models are more complex than those usually employed with this software, the speed of the model runs in RISKOptimizer (0.75–5 h for one run) would be restrictive for restoration scenarios that incorporate additional regions from higher resolution numerical models that are needed to support on-the-ground restoration decisions. In addition, we found the sensitivity of RISKOptimizer solutions to initial conditions limited our confidence that the model was converging on globally optimal solutions. At this time, therefore, we believe the need for computational efficiency and a more complete parameter search space would be better met by transferring the model to a compiled program language.

Although the ORO model is in the early stages of development, and is specifically designed for restoration of oysters in Chesapeake Bay, the framework could be transferred to other aquatic and marine systems, and adapted to support different aspects of an ecosystem approach to fisheries management. The ecological costs and benefits associated with fisheries management decisions could be assessed by varying fishing mortality or the minimum legal size and examining the influence of these actions on human use and ecological benefits. Also, the impact of different spatial strategies for managing fishing mortality could be assessed within the ORO model framework: the model could be formulated so that the negative impacts of fishing on ecosystem services could be minimized. The optimization approach could also be applied to abundant filter-feeding finfish that may influence ecosystem dynamics, although fish migrations make model implementation a more challenging, but not insurmountable, task. In any of these applications, the model could be expanded to assess the cost and potential benefits of achieving specific population abundance goals by either increasing restoration spending, or by varying restrictions on harvesting, or both. Finally, the ORO model could be used to assess the potential influence of climate change on restoration and management programs by forcing the hydrodynamic, water quality, and larval transport models with future projections of temperature, freshwa-

ter flow, and wind derived from global climate models. As such, this method of linking physical and biological models in an optimization framework has broad application for an ecosystem approach to management, from making tactical site-specific recommendations to guiding spatially explicit harvest policies to understanding and responding to the local impacts of global climate change.

ACKNOWLEDGMENTS

We thank Thomas Maslin, Thomas Wazniak, Javier Ordóñez, Mark Luckenbach, Donald Meritt, Chris Judy, and Victor Kennedy for their assistance and insights. This research was funded by the Keith Campbell Foundation for the Environment, the National Science Foundation (OCE-0424932, OCE-0829512), and the University of Maryland Center for Environmental Science. This is UMCES HPL contribution number 4337.

LITERATURE CITED

- Barnes, T. K., A. K. Volety, K. Chartier, F. J. Mazzotti, and L. Pearlstine. 2007. A habitat suitability index model for the eastern oyster (*Crassostrea virginica*), a tool for restoration of the Caloosahatchee Estuary, Florida. *Journal of Shellfish Research* 26:949–959.
- Boicourt, W. C. 1992. Influences of circulation processes on dissolved oxygen in the Chesapeake Bay. Pages 7–59 in D. E. Smith, M. Leffler, and G. Mackiernan, editors. *Oxygen dynamics in the Chesapeake Bay: a synthesis of recent research*. Maryland Sea Grant Publications, College Park, Maryland, USA.
- Brumbaugh, R. D., L. A. Sorabella, C. O. Garcia, W. J. Goldsborough, and J. A. Wesson. 2000. Making a case for community-based oyster restoration: an example from Hampton Roads, Virginia, USA. *Journal of Shellfish Research* 19:467–472.
- Calvo, G. W., M. W. Luckenbach, S. K. Allen, and E. M. Burreson. 2001. A comparative field study of *Crassostrea ariakensis* (Fujita 1913) and *Crassostrea virginica* (Gmelin 1791) in relation to salinity in Virginia. *Journal of Shellfish Research* 20:221–229.
- Cerco, C., and M. R. Noel. 2005. Assessing a ten-fold increase in the Chesapeake Bay native oyster population. Report to EPA Chesapeake Bay Program, Annapolis, Maryland, USA.
- Cerco, C. F., and M. R. Noel. 2007. Can oyster restoration reverse cultural eutrophication in Chesapeake Bay? *Estuaries and Coasts* 30:331–343.
- Choi, K.-S., D. H. Lewis, E. N. Powell, and S. M. Ray. 1993. Quantitative measurement of reproductive condition in the American oyster *Crassostrea virginica* (Gmelin), using an enzyme-linked immunosorbent assay (ELISA). *Aquaculture and Fisheries Management* 24:299–322.
- Coen, D. L., R. D. Brumbaugh, D. Bushek, R. Grizzle, M. W. Luckenbach, M. H. Posey, S. P. Powers, and S. G. Tolley. 2007. Ecosystem services related to oyster restoration. *Marine Ecology Progress Series* 341:303–307.
- Davis, H. C. 1958. Survival and growth of clam and oyster larvae at different salinities. *Biological Bulletin* 114:296–307.
- Davis, H. C., and A. Calabrese. 1964. Combined effects of temperature and salinity on development of eggs and growth of larvae of *M. mercenaria* and *C. virginica*. *Fishery Bulletin* 63:643–655.
- Fulford, R. S., D. L. Brietburg, R. I. E. Newell, W. M. Kemp, and M. Luckenbach. 2007. Effects of oyster population restoration strategies on phytoplankton biomass in Chesapeake Bay: a flexible modeling approach. *Marine Ecology Progress Series* 336:43–61.
- Grizzle, R. E., J. K. Greene, and L. D. Coen. 2008. Seston removal by natural and constructed intertidal Eastern Oyster

- (*Crassostrea virginica*) reefs: a comparison with previous laboratory studies, and the value of in situ methods. *Estuaries and Coasts* 31:1208–1220.
- Harding, J. M., and R. Mann. 2001. Oyster reefs as fish habitat: opportunistic use of restored reefs by transient fishes. *Journal of Shellfish Research* 20:951–959.
- Hobbs, R. J., and J. A. Harris. 2001. Restoration ecology: repairing the Earth's ecosystems in the new millennium. *Restoration Ecology* 9:239–246.
- Hofmann, E., S. Ford, E. Powell, and J. Klinck. 2001. Modeling studies of the effect of climate variability on MSX disease in eastern oyster (*Crassostrea virginica*) populations. *Hydrobiologia* 460:195–212.
- Holyoke, R. R. 2006. Biodeposition and biogeochemical processes in shallow, mesohaline sediments of Chesapeake Bay. Dissertation. University of Maryland, College Park, Maryland, USA.
- Hood, R. R., N. R. Bates, D. G. Capone, and D. B. Olson. 2001. Modeling the effect of nitrogen fixation on carbon and nitrogen fluxes at BATS. Deep Sea Research Part II: Topical Studies in Oceanography 48:1609–1648.
- Hood, R. R., H. V. Wang, J. E. Purcell, E. D. Houde, and L. W. Harding, Jr. 1999. Modeling particles and pelagic organisms in Chesapeake Bay: convergent features control plankton distributions. *Journal of Geophysical Research* 104: 1223–1243.
- Johnson, B. H., K. W. Kim, R. H. Heath, H. L. Butler, and B. B. Hsieh. 1991. Development and verification of a three-dimensional numerical hydrodynamic, salinity, and temperature model of the Chesapeake Bay. Technical Report HL-91-7. U.S. Army Engineer Waterways Experiment Station, Vicksburg, Mississippi, USA.
- Jordan, S. J., K. N. Greenhawk, C. B. McCollough, J. Vanisko, and M. L. Homer. 2002. Oyster biomass, abundance, and harvest in northern Chesapeake Bay: trends and forecasts. *Journal of Shellfish Research* 21:733–741.
- Kennedy, V. S. 1991. Eastern oyster *Crassostrea virginica*. Pages 3-1–3-20 in S. L. Funderburk, S. J. Jordan, J. A. Mihursky, and D. Riley, editors. Habitat requirements for Chesapeake Bay living resources. Chesapeake Bay Program, Annapolis, Maryland, USA.
- Klinck, J. M., E. E. Hofmann, E. N. Powell, and M. M. Deksheniaks. 2002. Impact of channelization on oyster production: a hydrodynamic-oyster population model for Galveston Bay, Texas. *Environmental Modeling and Assessment* 7:273–289.
- Li, M., L. Zhong, and W. C. Boicourt. 2005. Simulations of Chesapeake Bay estuary: Sensitivity to turbulence mixing parameterizations and comparison with observations. *Journal of Geophysical Research* 110(C12004). [doi: 10.1029/2004JC002585]
- Liddel, M. K. 2008. A von Bertalanffy based model for the estimation of oyster (*Crassostrea virginica*) growth on restored oyster reefs in Chesapeake Bay. Dissertation. University of Maryland, College Park, Maryland, USA.
- Lough, R. G. 1975. A reevaluation of the combined effects of temperature and salinity on survival and growth of bivalve larvae using response surface techniques. *Fishery Bulletin* 73: 86–94.
- Mann, R., and E. N. Powell. 2007. Why oyster restoration goals in the Chesapeake Bay are not and probably cannot be achieved. *Journal of Shellfish Research* 26(4):1–13.
- McCay, D. P. F., C. H. Peterson, J. T. DeAlteris, and J. Catena. 2003. Restoration that targets function as opposed to structure: replacing lost bivalve production and filtration. *Marine Ecology Progress Series* 264:197–212.
- National Oceanic and Atmospheric Administration. 2005. New priorities for the 21st century: NOAA's strategic plan. National Oceanic and Atmospheric Administration, Washington, D.C., USA.
- National Research Council Committee on Nonnative Oysters in the Chesapeake Bay. 2004. Nonnative oysters in the Chesapeake Bay. National Academies Press, Washington, D.C., USA.
- Newell, R. I. E., J. C. Cornwell, and M. S. Owens. 2002. Influence of simulated bivalve biodeposition and microphytobenthos on sediment nitrogen dynamics: a laboratory study. *Limnology and Oceanography* 47:1367–1379.
- Newell, R. I. E., T. R. Fisher, R. R. Holyoke, and J. C. Cornwell. 2005. Influence of eastern oysters on nitrogen and phosphorus regeneration in Chesapeake Bay, USA. Pages 93–120 in R. Dame and S. Olenin, editors. The comparative roles of suspension feeders in ecosystems. Volume 47. Springer, Dordrecht, The Netherlands.
- Newell, R. I. E., and E. W. Koch. 2004. Modeling seagrass density and distribution in response to changes in turbidity stemming from bivalve filtration and seagrass sediment stabilization. *Estuaries* 27:793–806.
- Newell, R. I. E., and C. J. Langdon. 1996. Mechanisms and physiology of larval and adult feeding. Page 734 in V. S. Kennedy, R. I. E. Newell, and A. E. Eble, editors. The Eastern Oyster, *Crassostrea virginica*. Maryland Sea Grant College, College Park, Maryland, USA.
- North, E. W., Z. Schlag, R. R. Hood, M. Li, L. Zhong, T. Gross, and V. S. Kennedy. 2008. Vertical swimming behavior influences the dispersal of simulated oyster larvae in a coupled particle-tracking and hydrodynamic model of Chesapeake Bay. *Marine Ecology Progress Series* 359:99–115.
- Powell, E. N., J. M. Klinck, E. E. Hofmann, E. A. Wilson-Ormond, and M. S. Ellis. 1995. Modeling oyster populations. V. Declining phytoplankton stocks and the population dynamics of American oyster (*Crassostrea virginica*) populations. *Fisheries Research* 24:199–122.
- Powell, E. N., J. N. Kraeuter, and K. A. Ashton-Alcox. 2006. How long does oyster shell last on an oyster reef? *Estuarine, Coastal and Shelf Science* 69:531–542.
- Pritchard, D. W. 1952. Salinity distribution and circulation in the Chesapeake Bay estuarine system. *Journal of Marine Research* 11:106–123.
- Rodney, W. S., and K. T. Paynter. 2006. Comparisons of macrofaunal assemblages on restored and non-restored oyster reefs in mesohaline regions of Chesapeake Bay in Maryland. *Journal of Experimental Marine Biology and Ecology* 335:39–51.
- Schubel, J. R., and D. W. Pritchard. 1987. A brief physical description of the Chesapeake Bay. Pages 1–32 in S. K. Majumdar, L. W. Hall, Jr., and H. M. Adams, editors. Contaminant problems and management of living Chesapeake Bay resources. The Pennsylvania Academy of Science, Easton, Pennsylvania, USA.
- Shen, J., and H. V. Wang. 2007. Determining the age of water and long-term transport time scale of the Chesapeake Bay. *Estuarine, Coastal and Shelf Science* 74:750–763.
- Sheng, Y. P. 1986. A three-dimensional mathematical model of coastal, estuarine, and lake currents using a boundary fitted grid. Report 585. Princeton, New Jersey, USA.
- Shumway, S. E. 1996. Natural environmental factors. Page 734 in V. S. Kennedy, R. I. E. Newell, and A. E. Eble, editors. The Eastern Oyster: *Crassostrea virginica*. Maryland Sea Grant Publication, College Park, Maryland, USA.
- Smith, G. F., D. G. Bruce, E. B. Roach, A. Hansen, R. I. E. Newell, and A. M. McManus. 2005. Assessment of recent habitat conditions of Eastern Oyster *Crassostrea virginica* bars in mesohaline Chesapeake Bay. *North American Journal of Fisheries Management* 25:1569–1590.
- Smith, G. F., K. N. Greenhawk, D. G. Bruce, E. B. Roach, and S. J. Jordan. 2001. A digital presentation of the Maryland oyster habitat and associated bottom types in the Chesapeake Bay (1974–1983). *Journal of Shellfish Research* 20:197–206.
- Volety, A. K., M. Savarese, S. G. Tolley, W. S. Arnold, P. Sime, P. Goodman, R. H. Chamberlain, and P. H. Doering.

2009. Eastern oysters (*Crassostrea virginica*) as an indicator for restoration of Everglades ecosystems. *Ecological Indicators* 9(special issue supplement 6):S120–S136.
- Vølstad, J. H., J. Dew, and M. Tarnowski. 2008. Estimation of annual mortality rates for eastern oysters (*Crassostrea virginica*) in Chesapeake Bay based on box counts and application of those rates for projection of population growth of *C. virginica* and *C. ariakensis*. *Journal of Shellfish Research* 27:525–533.
- Wang, D.-P. 1979. Subtidal sea level variations in the Chesapeake Bay and relations to atmospheric forcing. *Journal of Physical Oceanography* 9:413–421.
- Wang, H. V., and R. S. Chapman. 1995. Application of vertical turbulence closure schemes in the Chesapeake Bay circulation model: a comparative study. Pages 283–297 *in* Malcolm L. Spaulding and Ralph T. Cheng, editors. Proceedings of the 4th International Conference, San Diego, California, October 26–28, 1995. American Society of Civil Engineers, New York, New York, USA.
- Xu, J., S.-Y. Chao, R. R. Hood, H. V. Wang, and W. C. Boicourt. 2002. Assimilating high-resolution salinity data into a model of a partially mixed estuary. *Journal of Geophysical Research* 107(C7):3074. [doi: 10.1029/2001JC000626]
- Xu, J., and R. R. Hood. 2006. Modeling biogeochemical cycles in Chesapeake Bay with a coupled physical-biological model. *Estuarine Coastal and Shelf Science* 69:9–46.
- Xu, J., R. R. Hood, and S.-Y. Chao. 2005. A simple empirical optical model for simulating light attenuation variability in a partially mixed estuary. *Estuaries* 28:572–580.
- Zhong, L., and M. Li. 2006. Tidal energy fluxes and dissipation in the Chesapeake Bay. *Continental Shelf Research* 26:752–770.